A&A 491, 507–513 (2008)
DOI: 10.1051/0004-6361:200810272

Astronomy & Astrophysics

Progenitor mass of the type IIP supernova 2005cs

V. P. Utrobin[1,2] and N. N. Chugai[3]

[1] Max-Planck-Institut für Astrophysik, Karl-Schwarzschild-Str. 1, 85741 Garching, Germany
[2] Institute of Theoretical and Experimental Physics, B. Cheremushkinskaya St. 25, 117218 Moscow, Russia
e-mail: utrobin@itep.ru
[3] Institute of Astronomy of Russian Academy of Sciences, Pyatnitskaya St. 48, 109017 Moscow, Russia

Received 27 May 2008 / Accepted 29 August 2008

ABSTRACT

Context. The progenitor mass of type IIP supernova can be determined from either hydrodynamic modeling of the event or pre-explosion observations.
Aims. To compare these approaches, we determine parameters of the sub-luminous supernova 2005cs and estimate its progenitor mass.
Methods. We compute the hydrodynamic models of the supernova to describe its light curves and expansion velocity data.
Results. We estimate a presupernova mass of $17.3 \pm 1\ M_\odot$, an explosion energy of $(4.1 \pm 0.3) \times 10^{50}$ erg, a presupernova radius of $600 \pm 140\ R_\odot$, and a radioactive ^{56}Ni mass of $0.0082 \pm 0.0016\ M_\odot$. The derived progenitor mass of SN 2005cs is $18.2 \pm 1\ M_\odot$, which is in-between those of low-luminosity and normal type IIP supernovae.
Conclusions. The obtained progenitor mass of SN 2005cs is higher than derived from pre-explosion images. The masses of four type IIP supernovae estimated by means of hydrodynamic modeling are systematically higher than the average progenitor mass for the $9-25\ M_\odot$ mass range. This result, if confirmed for a larger sample, would imply that a serious revision of the present-day view on the progenitors of type IIP supernovae is required.

Key words. stars: supernovae: general – stars: supernovae: – individual: SN 2005cs

1. Introduction

Type IIP supernovae (SNe IIP) originate presumably in main-sequence stars of the mass range of $9-25\ M_\odot$ (Heger et al. 2003). If this is the case, the predicted rate of SNe IIP should follow the Salpeter initial mass function with half of events occurring for stars of mass below $13\ M_\odot$. This conjecture requires confirmation by means of the determination of progenitor mass for an extended sample of SNe IIP.

There are two ways to recover the progenitor mass of SN IIP on the main sequence. The first method is detection of the pre-supernova (pre-SN) in archival images of the host galaxy. The estimated flux and color index of the detected pre-SN is then converted into a stellar mass using the flux and color index predicted by stellar evolution models. Data for the available directly identified progenitors in the compilation of Li et al. (2007) indicate that for eight SNe IIP the progenitor masses have been estimated in this way, and for six SNe IIP, upper limits to the progenitor mass have been found.

An alternative approach to the mass determination involves hydrodynamic modeling of light curves and expansion velocities for the well-observed SNe IIP. Combining the ejecta mass derived from the hydrodynamic modeling with the mass of the neutron star and the mass lost by the stellar wind provides us with the mass estimate of the progenitor. Henceforth, the progenitor mass determined by this method is referred to as the "hydrodynamic mass". At present, the hydrodynamic mass is measured only for three SNe IIP: the peculiar type IIP SN 1987A (Woosley 1988; Blinnikov et al. 2000; Utrobin 2005), the normal type IIP SN 1999em (Baklanov et al. 2005; Utrobin 2007), and the low-luminosity type IIP SN 2003Z (Utrobin et al. 2007). The small amount of SN IIP events with the measured hydrodynamic mass is related to the fact that the hydrodynamic modeling requires a complete multi-band photometry at both the plateau and the radioactive tail, and spectra of sufficient quality.

There are only a few other SNe IIP that also meet these requirements. Among these is the sub-luminous type IIP SN 2005cs (Pastorello et al. 2006). On the basis of its luminosity and expansion velocities, this SN is intermediate between the low-luminosity and normal SNe IIP. Parameters of SN 2005cs are of considerable interest for two major reasons: (1) this SN is expected to have intermediate parameters, which would be interesting to check; (2) the pre-SN was detected in the pre-explosion images and its progenitor mass was estimated by several groups (Maund et al. 2005; Li et al. 2006; Eldridge et al. 2007) providing an opportunity to compare different mass estimates.

In the paper, we perform hydrodynamic modeling of SN 2005cs to recover the parameters: ejecta mass, explosion energy, pre-SN radius, and radioactive ^{56}Ni mass. We start with the description of the model and observational data used and then present the results of the hydrodynamic modeling for SN 2005cs (Sect. 2). In Sect. 3, we present additional arguments in favor of our choice of pre-SN models. Possible uncertainties in the hydrodynamic mass of SN 2005cs are analyzed (Sect. 4), and finally the implications of hydrodynamically studied objects for the origin of SNe IIP are discussed (Sect. 5).

We adopt an explosion date on June 27.5 UT (JD 2 453 549) and a distance of 8.4 Mpc following Pastorello et al. (2006), and a reddening $E(B-V) = 0.12$ taken from Li et al. (2006).

2. Optimal hydrodynamic model

The hydrodynamic model applied to SN 2005cs is essentially the same as used before for SN 1999em (Utrobin 2007). The

pre-SN structure is set to be a non-evolutionary model of a red supergiant (RSG) star (but see Sect. 3). The chemical composition of the hydrogen envelope is solar. Although this might be a simplification, there is no observational evidence that the hydrogen abundance in the atmosphere of the RSG, e.g. α Ori, differs notably from solar (Harper et al. 2001). The effect of the variation in the surface abundances on the SN IIP light curve was studied before, and it was found that even a significant change in the hydrogen abundance of outer layers only weakly affects the light curve (Utrobin 2007). The light curve of the SN 2005cs model of hydrogen abundance $X = 0.65$ and helium abundance $Y = 0.33$, predicted for an 18 $M_\odot$ star with initial solar composition (Heger 1998), is almost indistinguishable from the case of solar composition. The inner layers of the ejecta are mixed with the helium core in the same way as in the model for SN 1999em.

We refer to the hydrodynamic model as being the optimal one, in terms of an "eye-fit" to the observational light curve and the evolution of photospheric velocity. In general, a numerical optimization procedure could be developed to complete the search for the best-fit model. However, at present it would require an enormous amount of computational time that would be unjustified because the error of eye-fit is far less than the error introduced by uncertainties in the distance and interstellar extinction. The search for the optimal model of SN 2005cs uses the hydrodynamic model behavior in parameter space studied earlier in detail (Utrobin 2007). The ^{56}Ni mass is determined empirically from the comparison of the R-band luminosity of SN 2005cs at the radioactive tail with that of SN 1987A. For the adopted distance and reddening, the R-values at the age of 250–300 days (Tsvetkov et al. 2006) correspond to the ^{56}Ni mass of 0.0082 $M_\odot$.

The observed bolometric light curve of SN 2005cs is recovered from *UBVRI* photometry (Pastorello et al. 2006; Tsvetkov et al. 2006) using a black-body approximation for the SN radiation, while expansion velocities at the photosphere were taken from Pastorello et al. (2006).

The dependence of the light curve at the initial adiabatic cooling stage and the plateau phase on SN parameters provides us with a toolkit to search for the optimal model in parameter space. The obtained model of SN 2005cs is characterized by the ejecta mass $M_{\rm env} = 15.9\ M_\odot$, the explosion energy $E = 4.1 \times 10^{50}$ erg, and the pre-SN radius $R_0 = 600\ R_\odot$ with the ^{56}Ni mass $M_{\rm Ni} = 0.0082\ M_\odot$. The ejecta mass combined with the neutron star mass results in the pre-SN mass of 17.3 $M_\odot$.

The optimal pre-SN density structure is shown in Fig. 1 and the chemical composition in Fig. 2. The helium core is mixed with the hydrogen envelope so that the hydrogen abundance increases linearly with mass in the inner 9 $M_\odot$. We adopt the helium-core mass of 5.4 $M_\odot$, which corresponds to the $\approx$18 $M_\odot$ progenitor (Hirschi et al. 2004). We note that the basic SN parameters are insensitive to the helium-core mass (Utrobin et al. 2007). In the freely expanding envelope, the hydrogen is mixed downward to 300 km s^{-1}, while the radioactive ^{56}Ni is mixed outward to 610 km s^{-1} (Fig. 3).

The observed bolometric light curve is reproduced by our optimal model (Fig. 4). A small disparity between model and observations at the radioactive tail is probably caused by the black-body approximation applied to the reconstruction of the observed bolometric light curve. This approximation is certainly rough at the nebular epoch. We note that the ^{56}Ni mass was derived from the comparison of the R-band luminosities of SN 2005cs and SN 1987A at similar nebular epochs.

Although the one-group approximation for radiation transfer prevents us from achieving a detailed description of the spectral energy distribution, our model does reproduce the general magnitude of the broad-band photometry, although the match is not precise. Both the observed and calculated B light curves (Fig. 5a) show an initial peak related to the cooling of hot outer layers of shocked ejecta. The amplitude and width of this peak is sensitive to the structure of the outermost rarefied layers of the pre-SN envelope, and the density structure shown in Fig. 1 is optimal in this sense. The later ($t > 50$ days) behavior of the flux in B band is poorly reproduced because the black-body approximation of the model spectrum in the $\lambda < 4500$ Å range is too crude at the plateau stage. Fortunately, this discrepancy does not affect the model fit to the bolometric light curve because of a small contribution of the B band to the bolometric luminosity at this stage. The calculated V and R light curves for this model describe satisfactorily observations (Figs. 5b and c). The computed evolution of the photospheric velocity is also consistent with observations (Fig. 5d), supporting the detailed hydrodynamic properties of the model ejecta, in particular, the density distribution in the SN envelope (Fig. 3).

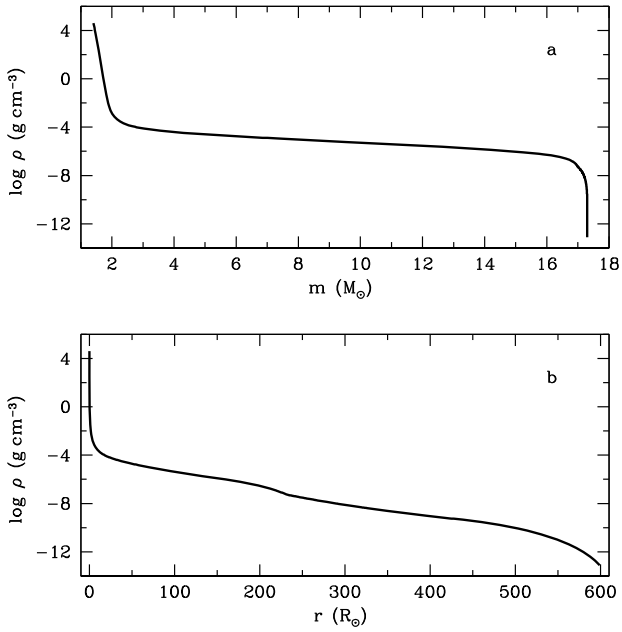

Fig. 1. Density distribution as a function of interior mass **a**) and radius **b**) for the optimal pre-SN model. The central core of 1.4 $M_\odot$ is omitted.

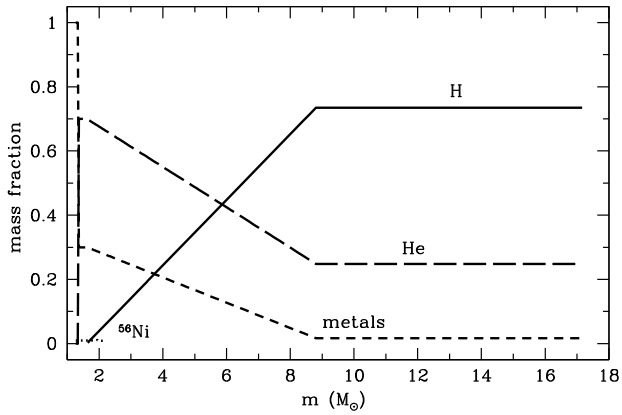

Fig. 2. The mass fraction of hydrogen (*solid line*), helium (*long dashed line*), heavy elements (*short dashed line*), and radioactive ^{56}Ni (*dotted line*) in the ejecta of the optimal model.

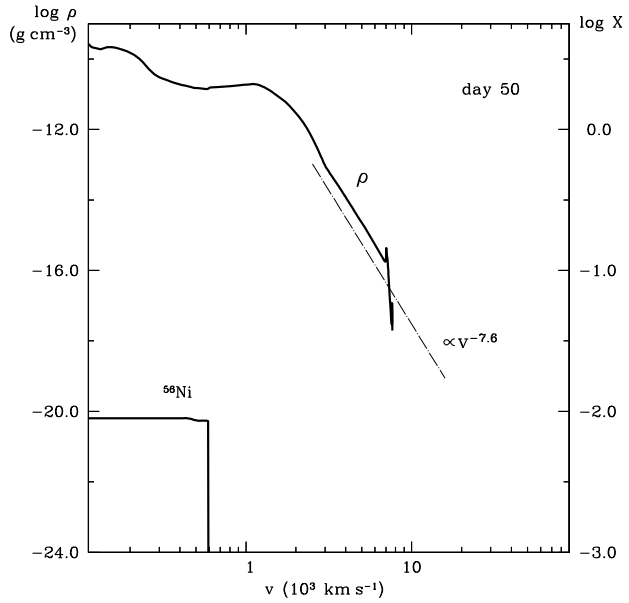

Fig. 3. The density and the ^{56}Ni mass fraction as a function of the velocity for the optimal model at $t = 50$ days. *Dash-dotted line* is the density distribution fit $\rho \propto v^{-7.6}$.

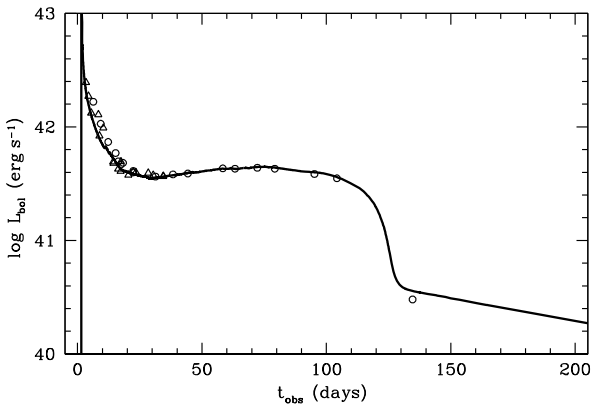

Fig. 4. Comparison of the calculated bolometric light curve of the optimal model (*solid line*) with the bolometric data of SN 2005cs evaluated from the photometric observations of Pastorello et al. (2006) (*open triangles*) and Tsvetkov et al. (2006) (*open circles*).

To estimate a measure of uncertainty in the derived physical parameters, we investigate the sensitivity of the optimal model to observational values. We adopt the following relative changes in the observational values: 20% in the bolometric luminosity, 5% in the photospheric velocity, and 5% in the plateau duration. Using the auxiliary hydrodynamic models in the vicinity of the optimal model, we transform the adopted changes into changes in the pre-SN radius of $\pm 140\ R_\odot$, the ejecta mass of $\pm 1\ M_\odot$, the explosion energy of $\pm 0.3 \times 10^{50}$ erg, and the ^{56}Ni mass of $\pm 0.0016\ M_\odot$. Given the errors in the observational values, these relations can be used to derive the errors in the physical parameters. The adopted relative changes in the observed values are close to their typical errors. We therefore consider the derived changes in the physical parameters of SN 2005cs to represent the typical uncertainties in these values.

3. Why non-evolutionary presupernova model?

Although our non-evolutionary pre-SN model closely resembles the massive RSG star by the heterogeneous core-envelope

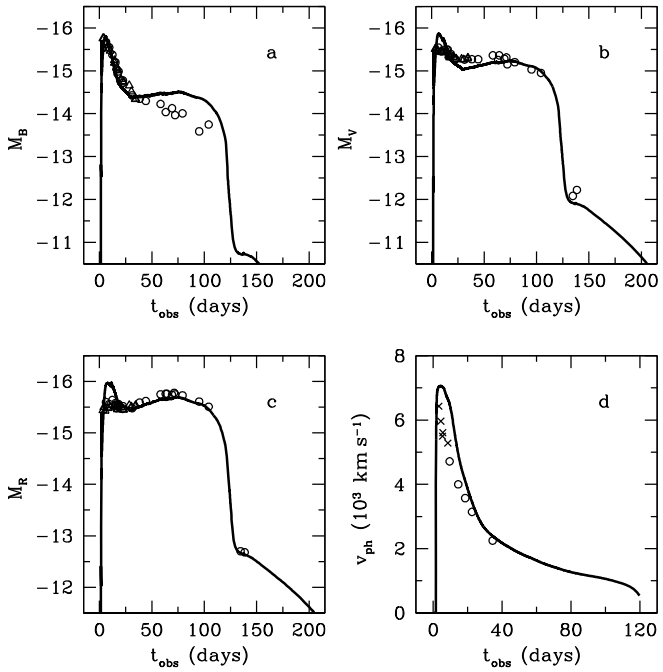

Fig. 5. Optimal hydrodynamic model. Panel **a)**: the calculated B light curve (*solid line*) compared with the observations of SN 2005cs obtained by Pastorello et al. (2006) (*open triangles*) and Tsvetkov et al. (2006) (*open circles*). Panels **b)** and **c)**: the same as panel **a)** but for the V and R light curves. Panel **d)**: calculated photospheric velocity (*solid line*) is compared with photospheric velocities estimated from absorption minima of the He I 5876 Å line (*crosses*) and the Fe II 5169 Å line (*open circles*) measured by Pastorello et al. (2006).

structure, the extended radius, and the helium-core mass, it omits a sharp jump in density and chemical composition between the helium core and hydrogen envelope, which is characteristic of the evolutionary model. A question may then arise: why not use evolutionary pre-SN. The answer is that the assumption of a smooth transition from the helium core to the hydrogen envelope in the non-evolutionary pre-SN is dictated by two major facts. First, the explosion of the evolutionary model generally fails to reproduce the light curve of SN IIP in detail, as became clear after SN 1987A (cf. Woosley 1988). Second, the Hα profile in the SN 1987A spectra provides clear evidence of hydrogen mixing deep down inside the helium core. We note that in 2D simulations the shock propagation produces Rayleigh-Taylor (RT) mixing between the oxygen and helium-core material, and between the helium-core matter and the hydrogen envelope (Herant & Benz 1991; Müller et al. 1991; Kifonidis et al. 2003, 2006).

In general, a self-consistent hydrodynamic model of the explosion of the evolutionary RSG star should be three-dimensional in considering both the hydrodynamic flow and radiation transfer. Unfortunately, this approach cannot presently be realized. We therefore accounted for 3D effects in our 1D simulations by adopting a non-evolutionary pre-SN with density and chemical composition jumps that had been smoothed presumably by the RT mixing between the helium core and the hydrogen envelope. This approach was justified because the RT mixing occurs before the shock breakout and does not affect the light curve directly.

Here we propose that a pre-SN has an evolutionary density structure and chemical composition. We constructed the hydrostatic configuration, which reproduced the main features of evolutionary pre-SN models neglected before, namely the dense

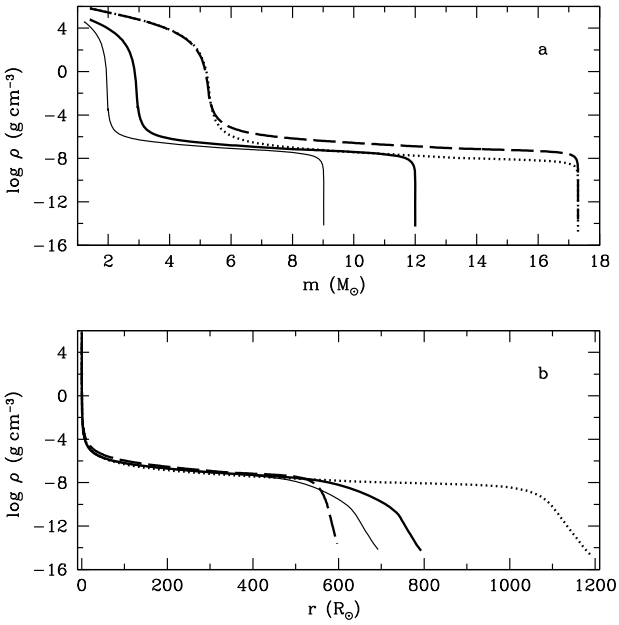

Fig. 6. Density distribution as a function of interior mass **a)** and radius **b)** for the evolutionary pre-SNe (Table 1): model EM1 (*dotted line*), model EM2 (*dashed line*), model EM3 (*thick solid line*), and model EM4 (*thin solid line*).

helium core with a sharp density gradient and the chemical composition jump at its boundary. We refer to this pre-SN model as the "evolutionary model". Four representative models with a dense helium core and extended hydrogen envelope (Fig. 6) were considered. Their parameters are listed in Table 1, i.e. the pre-SN radius, ejecta mass, explosion energy, total ^{56}Ni mass, helium-core mass, pre-SN mass, and surface hydrogen and helium abundances. The helium-core masses are typical of massive RSG stars (Hirschi et al. 2004; Garcia-Berro et al. 1997). The first two hydrodynamic models EM1 and EM2 are similar to the optimal model in the basic parameters but model EM1 differs in the initial radius. The remaining two models EM3 and EM4 are less massive than the optimal model and their masses are close to the progenitor mass of SN 2005cs estimated from the pre-explosion images of the galaxy M 51 (see Sect. 4). We consider also the mixed models EM3 and EM4 in which the helium core is mixed by the hydrogen envelope – in the same way as the optimal model is mixed (Fig. 2) – in the inner 4.7 $M_\odot$ and 2.8 $M_\odot$, respectively.

First of all, we see that the explosion of the evolutionary model produces the dome-shaped light curve without a steep transition to the radioactive tail (Figs. 7a–c). We note that the steep decline in luminosity at the end of the plateau is a characteristic of all SNe IIP. The dome shape of the light curve for the evolutionary model is related to the almost flat density distribution in the hydrogen envelope (Fig. 6). A step-like bump in the light curve at the transition to the radioactive tail is caused by the dense helium core (Fig. 6). We note that mixing in models EM3 and EM4 does not remove but modifies the step-like feature (Figs. 7b and c). The fact that this bump is never observed in SNe IIP indicates that the density jump between the dense helium core and flat hydrogen envelope is smoothed and, consequently, the inner SN ejecta is strongly mixed.

The hydrodynamic model EM1 with an initial radius of 1200 $R_\odot$, close to that of the evolutionary pre-SN (Heger 1998), predicts an unacceptably high luminosity, long plateau (Fig. 7a), and low photospheric velocity during the early epoch $t < 10$ days

Table 1. Hydrodynamic models for evolutionary presupernovae.

Model	R_0 ($R_\odot$)	$M_{\rm env}$ ($M_\odot$)	E (10^{50} erg)	$M_{\rm Ni}$ (10^{-2} $M_\odot$)	$M_{\rm He}^{\rm core}$ ($M_\odot$)	$M_{\rm pre-SN}$ ($M_\odot$)	X	Y
EM1	1200	15.9	4.1	0.82	5.4	17.3	0.65	0.33
EM2	600	15.9	4.1	0.82	5.4	17.3	0.65	0.33
EM3	800	10.6	1.5	0.82	3.0	12.0	0.65	0.33
EM4	700	7.8	1.4	0.82	2.0	9.0	0.65	0.33

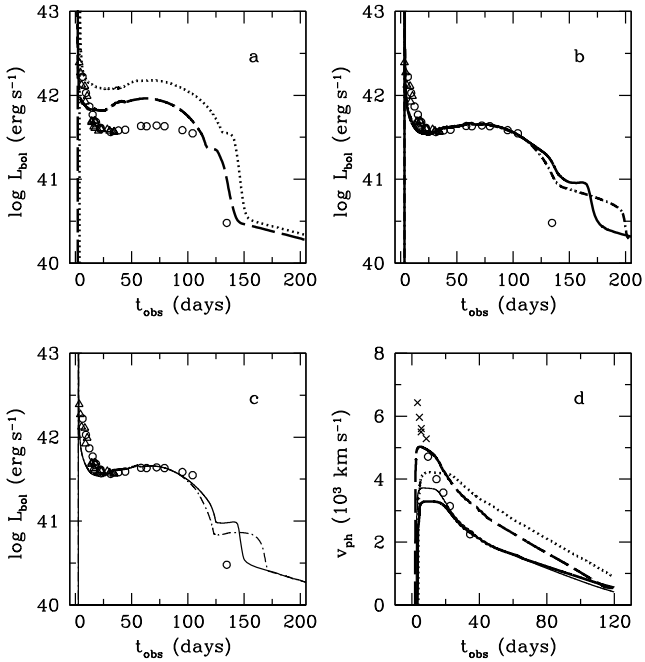

Fig. 7. Bolometric light curve **a)**, **b)**, and **c)** and photospheric velocity **d)** of the hydrodynamic models in Table 1 compared with the empirical data of SN 2005cs (see legends of Figs. 4 and 5 for details). *Dotted line* is model EM1, *dashed line* is model EM2, *thick solid line* is model EM3, and *thin solid line* is model EM4. Mixed models EM3 and EM4 are shown by the corresponding *dotted-dashed lines* in panels **b)** and **c)**.

(Fig. 7d). Model EM2 with the smaller initial radius, as expected, is characterized by lower luminosity, but remains too luminous (Fig. 7a) and has low photospheric velocity at the early epoch $t < 7$ days (Fig. 7d). The reduction in radius would produce a reasonable luminosity at the early plateau stage, but this model would have too low luminosity at the late plateau stage. We therefore conclude that the replacement of the non-evolutionary pre-SN in the optimal model by the evolutionary pre-SN cannot produce a reasonable fit to the observational data.

Models EM3 and EM4 of lower mass and explosion energy could reproduce the observed plateau luminosity for an appropriate choice of initial radius (Figs. 7b and c). However, a full description of the light curve cannot be attained for either the 12 $M_\odot$ or 9 $M_\odot$ pre-SNe. The photospheric velocity at the early stage in these models becomes unacceptably low (Fig. 7d), which is another reason why evolutionary models have to be modified significantly to attain a reasonable fit to observational data. Remarkably, all evolutionary models fail to reproduce the width of the initial peak. We therefore conclude that there is no set of the basic parameters for the 9–18 $M_\odot$ progenitors that can reproduce the observations of SN 2005cs in the frame of the 1D explosion of the evolutionary pre-SNe.

4. Progenitor mass

To derive the main-sequence mass of the SN 2005cs progenitor, the pre-SN mass needs to be combined with the mass lost during the hydrogen and helium burning stages. The mass lost at the hydrogen burning stage is taken to be $\approx 0.25\ M_\odot$, the average value between the masses lost in the 15 $M_\odot$ and 20 $M_\odot$ evolutionary models of non-rotating stars developed by Meynet et al. (2003), who assumed the theoretical mass-loss rate provided by Vink et al. (2001).

The mass lost at the helium burning stage can be estimated from the stage duration, which is a function of the initial mass M and mass-loss rate $\dot{M}$ adopted for the RSG stage. We adopt the duration of the helium burning stage from Meynet et al. (2003). The dependence of the mass-loss rate $\dot{M}$ on M was taken from Chevalier et al. (2006), who used $\dot{M}$ values from de Jager et al. (1988). We also used the calibration $\dot{M} = 1.5 \times 10^{-6}\ M_\odot\ \mathrm{yr}^{-1}$ for the RSG with a main-sequence star $M = 22\ M_\odot$, on the basis of the SN 1999em study (Chugai et al. 2007). The derived mass lost at the RSG stage was 0.6 $M_\odot$. The total mass lost by the stellar wind was $\approx 0.85\ M_\odot$, and the main-sequence mass of the progenitor was 18.2 $M_\odot$.

The mass of the SN 2005cs progenitor was estimated from archival images of the galaxy M 51 taken by the Advanced Camera for Surveys of the *Hubble Space Telescope* (*HST*) and from near-infrared images acquired by the Near Infrared Camera and Multi-Object Spectrometer on board *HST* in *JHK* bands. We note that the progenitor was detected only in the *I*-band image; in other bands, only upper limits to fluxes were obtained. From these data, Maund et al. (2005) derived a progenitor mass of $9^{+3}_{-2}\ M_\odot$, Li et al. (2006) reported a progenitor mass of $10 \pm 3\ M_\odot$, while Eldridge et al. (2007) derived a progenitor mass of between 6 $M_\odot$ and 8 $M_\odot$. These estimates therefore propose a 6−13 $M_\odot$ range for the progenitor mass of SN 2005cs.

The above mass estimates are significantly lower than our hydrodynamic mass. The disagreement is serious and requires an explanation. Our hydrodynamic model for SN IIP (Utrobin 2004) can be checked by comparison with the independent model of Blinnikov et al. (1998). In the case of the normal type IIP SN 1999em, both codes produce similar ejecta mass by assuming the same distance (Baklanov et al. 2005; Utrobin 2007). We explored crucial model assumptions that might minimize the ejecta mass. One critical point is the degree of mixing between the hydrogen envelope and helium core. We found that the minimal mass was produced, if complete mixing occurred. In this case, the ejecta mass of the hydrodynamic model could be reduced by about 0.5 $M_\odot$. Another uncertainty was related to the incompleteness of the line list used in the line-opacity calculations. By studying this issue using the latest line list of Kurucz with $\approx 6.2 \times 10^7$ observed and predicted lines, it was found to provide only negligible effect, which may cause the mass decrease by the value of the order of 0.1 $M_\odot$. Both uncertainties implied a lower limit for the hydrodynamic progenitor mass as low as 17.6 $M_\odot$, which is higher than the upper limit of 13 $M_\odot$ recovered from the pre-explosion images of SN 2005cs.

5. Discussion and conclusions

The primary goal of this study was to determine parameters of the sub-luminous type IIP SN 2005cs by means of hydrodynamic modeling. We have estimated a pre-SN mass of $17.3 \pm 1\ M_\odot$, explosion energy of $(4.1 \pm 0.3) \times 10^{50}$ erg, pre-SN radius of $600 \pm 140\ R_\odot$, and ^{56}Ni mass of $0.0082 \pm 0.0016\ M_\odot$. Using conservative assumptions about the mass-loss rate at the hydrogen and helium burning stages, we estimate the main-sequence progenitor mass of 17.2−19.2 $M_\odot$.

Table 2. Hydrodynamic models for SN 1987A, SN 1999em, SN 2003Z, and SN 2005cs.

SN	R_0 ($R_\odot$)	$M_{\rm env}$ ($M_\odot$)	E (10^{51} erg)	$M_{\rm Ni}$ ($10^{-2}\ M_\odot$)	Z	$v_{\rm Ni}^{\rm max}$ (km s^{-1})	$v_{\rm H}^{\rm min}$ (km s^{-1})
87A	35	18	1.5	7.65	0.006	3000	600
99em	500	19	1.3	3.60	0.017	660	700
03Z	229	14	0.245	0.63	0.017	535	360
05cs	600	15.9	0.41	0.82	0.017	610	300

Hydrodynamic models for four SNe IIP listed in Table 2 are characterized by the pre-SN radius, the ejecta mass, the explosion energy, the total ^{56}Ni mass, the surface abundance of heavy elements, the maximum velocity of nickel, and the minimum velocity of the hydrogen-rich envelope. The major parameters of SN 2005cs – the ejecta mass, the explosion energy, and the ^{56}Ni mass – are intermediate between those of the low-luminosity type IIP SN 2003Z (Utrobin et al. 2007) and the normal type IIP SN 1999em (Utrobin 2007) in qualitative agreement with their luminosities. At present, there are therefore four SNe IIP that have parameters determined by hydrodynamic modeling. For these objects, the explosion energy and ^{56}Ni mass correlate with the progenitor mass (Fig. 8). This is consistent with the empirical relation between the explosion energy and ^{56}Ni mass found by Nadyozhin (2003) for normal SNe IIP.

Despite the uncertainties in hydrodynamic modeling, the disparity between the hydrodynamic mass of the SN 2005cs progenitor and the mass estimated from the pre-explosion images is significant. This difference could be decreased by including the effects of the pre-SN light absorption in a hypothetical dusty circumstellar shell. However, this issue requires careful consideration, which is beyond the scope of our paper. We note only that this conjecture has a number of observational implications need to be to verified. The presence of the dense dusty shell around pre-SN should produce strong Na I absorption lines in the SN IIP spectrum at the photospheric epoch. In the case of a normal SN IIP and normal pre-SN wind without a dense circumstellar shell, the predicted Na I absorptions are weak and probably not observable (Chugai & Utrobin 2008). In addition, the interaction of the SN ejecta with the dense circumstellar shell should produce an outburst of radio and X-ray emission at an age of about $\sim 10^2$ days. The most apparent effect of the light absorption in the dusty circumstellar shell should be a large $J - K$ color index of the pre-SN. For instance, we have found that the pre-SN light absorption, required to allow massive progenitor implied by both the pre-explosion I value and upper limits in other bands for SN 2005cs, suggests a large color index $J - K \approx 2.5$ mag, compared with the intrinsic $J - K$ index of 0.7−1 mag for typical galactic K-M supergiants (Elias et al. 1985). In this regard, it is noteworthy that the type IIP SN 2008bk in the nearby galaxy NGC 7793 with available *JK* photometry of the progenitor was found to have a moderate color index $J - K \approx 1$ mag (Maoz & Mannucci 2008) which indicates little (if any) absorption. The observational and hydrodynamic studies of this supernova would be of significant importance in clarifying the serious and challenging problem of the progenitor mass of SN 2005cs and in general SNe IIP.

The number of SNe IIP with measured hydrodynamic masses is too small to be able to analyze in detail and draw reliable conclusions about their mass distribution. However, the

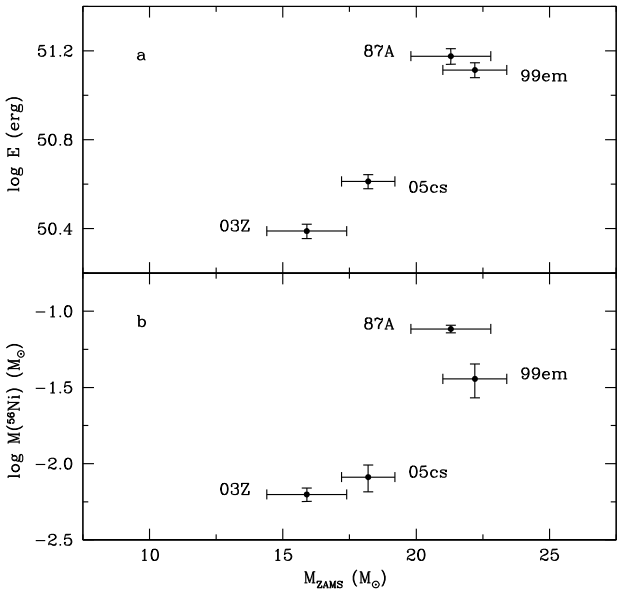

Fig. 8. Explosion energy **a**) and ^{56}Ni mass **b)** versus hydrodynamic progenitor mass for four core-collapse SNe.

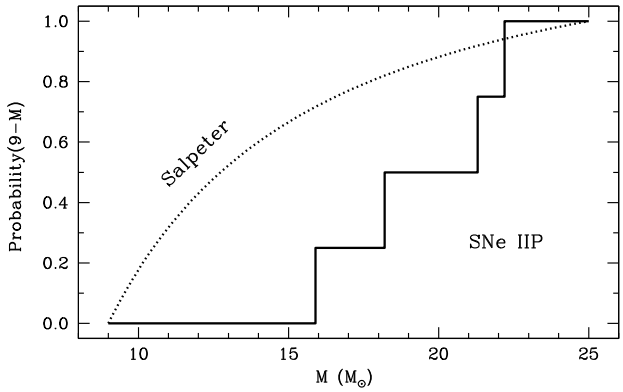

Fig. 9. Cumulative "Salpeter" distribution of SN IIP progenitors in the 9−25 $M_\odot$ mass range and the distribution of hydrodynamic progenitor masses of four SNe IIP.

hydrodynamic progenitor masses do appear to be systematically higher than if SNe IIP had originated from the range of 9−25 $M_\odot$, assuming a Salpeter initial mass function. This is clearly demonstrated by the comparison of the SNe IIP mass distribution, calculated by assuming a Salpeter initial mass function in the 9−25 $M_\odot$ mass range, with the mass distribution of four SNe IIP of known hydrodynamic mass (Fig. 9). Despite the small number of events, the significance of the difference between the two distributions is high: the probability that the four SNe occurred at random in the mass range of 15−25 $M_\odot$ is only 0.01. This indicates that either the 1D model of the SN explosion overestimates the ejecta mass, or the outcome of the core collapse of 9−15 $M_\odot$ stars differs markedly from that of SNe IIP observed until now.

To study the first possibility, we would require 3D radiation hydrodynamics modeling, which is not possible at present. While we cannot readily ascertain any 3D effect that might reduce the required ejecta mass, apparent 3D effects do exist that could increase the hydrodynamic mass. Indeed, the RT mixing between the helium core and the hydrogen envelope is expected to produce heterogeneous ejecta consisting of helium clumps embedded in the hydrogen background. This structure should reduce unavoidably the average opacity of the hydrogen-rich matter. As a result, the ejecta mass required to reproduce the observations should increase. This could counterbalance other possible effects that might reduce the ejecta mass. We believe therefore that the 3D hydrodynamic simulations are unlikely to reduce significantly the SN IIP progenitor masses recovered from the 1D modeling. The situation could be eventually clarified by 3D modeling of the SN IIP explosion.

Alternatively, the disparity between the two distributions in Fig. 9 is real. In this case two explanations could be invoked: (1) 9−15 $M_\odot$ stars produce faint, still undetectable SNe IIP, i.e. we have a selection effect; (2) core collapse of stars from this mass range does not produce an SN event at all. In the latter case, the fate of the star may be silent collapse with a neutron star residing inside the stellar envelope, i.e. a Thorne-Żytkow object (Thorne & Żytkow 1975). If this is the case, the neutron star may eventually grow into a black hole of mass as high as ∼15 $M_\odot$ due to the rapid (∼10^2 years) accretion of the stellar envelope (Bisnovatyi-Kogan & Lamzin 1984).

The second option appears, however, to be unlikely, because it implies that, apart from double neutron stars (DNS) originating from 9−25 $M_\odot$ stars, there should be a comparable number of binaries with a neutron star in combination with a black hole (NSBH binaries). Assuming that the production rate of DNS and NSBH binaries from 9−25 $M_\odot$ stars is determined by the random pairing of stars with the Salpeter initial mass function and that 9−15 $M_\odot$ stars produce black holes, we expect the relative rate of formation of these binaries to be DNS:NSBH = 1:0.85 for 9−25 $M_\odot$ stars. This ratio is in an apparent contradiction with the fact that eight DNS in the Galaxy are known (Ihm et al. 2006, and references therein) and no NSBH binary has yet been discovered. The probability of a random realization of this situation is only 1.5×10^{-5}, i.e. sufficiently small to be able to exclude the second option that stars in the mass range of 9−15 $M_\odot$ end their lifes as black holes.

We propose that the core collapse of 9−15 $M_\odot$ stars should produce a neutron star and the remaining stellar matter ejected as a result of a faint SN event. This picture predicts that the rate of faint SNe IIP should be comparable with the combined rate of normal (e.g., SN 1999em), sub-luminous (e.g., SN 2005cs), and low-luminosity (e.g., SN 2003Z) SNe IIP. A detection of the extended class of faint SNe IIP, or non-detection at a low flux level, could verify this scenario for 9−15 $M_\odot$ stars. It is interesting that some known transient events, e.g. SN 1997bs (Van Dyk et al. 2000), optical transient M 85 OT2006-1 (Pastorello et al. 2007), and SN 2008S (Prieto et al. 2008) might belong to the proposed category of faint SNe related to the mass range of 9−15 $M_\odot$.

Acknowledgements. V.U. is very grateful to Wolfgang Hillebrandt for the excellent opportunity to work at the MPA. We thank the referee John Eldridge for careful reading of the manuscript and helpful comments.

References

Baklanov, P. V., Blinnikov, S. I., & Pavlyuk, N. N. 2005, Astron. Lett., 31, 429
Bisnovatyi-Kogan, G. S., & Lamzin, S. A. 1984, Sov. Astron., 28, 187
Blinnikov, S. I., Eastman, R., Bartunov, O. S., Popolitov, V. A., & Woosley, S. E. 1998, ApJ, 496, 454
Blinnikov, S., Lundqvist, P., Bartunov, O., Nomoto, K., & Iwamoto, K. 2000, ApJ, 532, 1132
Chevalier, R. A., Fransson, C., & Nymark, T. K. 2006, ApJ, 641, 1029
Chugai, N. N., & Utrobin, V. P. 2008, Astron. Lett., 34, 589
Chugai, N. N., Chevalier, R. A., & Utrobin, V. P. 2007, ApJ, 662, 1136
de Jager, C., Nieuwenhuijzen, H., van der Hucht, K. A. 1988, A&AS, 72, 259
Eldridge, J. J., Mattila, S., & Smartt, S. J. 2007, MNRAS, 376, L52
Elias, J. H., Frogel, J. A., & Humphreys, R. M. 1985, ApJS, 57, 91

Garcia-Berro, E., Ritossa, C., & Iben, I. Jr. 1997, ApJ, 485, 765
Harper, G. M., Brown, A., & Lim, J. 2001, ApJ, 551, 1073
Heger, A. 1998, The presupernova evolution of rotating massive stars. Ph.D. Thesis, Technische Universität München
Heger, A., Fryer, C. L., Woosley, S. E., Langer, N., & Hartmann, D. H. 2003, ApJ, 591, 288
Herant, M., & Benz, W. 1991, ApJ, 370, L81
Hirschi, R., Meynet, G., & Maeder, A. 2004, A&A, 425, 649
Ihm, C. M., Kalogera, V., & Belczynski, K. 2006, ApJ, 652, 540
Kifonidis, K., Plewa, T., Scheck, L., Janka, H.-Th., & Müller, E. 2003, A&A, 408, 621
Kifonidis, K., Plewa, T., Scheck, L., Janka, H.-Th., & Müller, E. 2006, A&A, 453, 661
Li, W., Van Dyk, S. D., Filippenko, A. V., et al. 2006, ApJ, 641, 1060
Li, W., Wang, X., Van Dyk, S. D., et al. 2007, ApJ, 661, 1013
Maoz, D., & Mannucci, F. 2008, ATel, 1464
Meynet, G., & Maeder, A. 2003, A&A, 404, 975
Maund, J. R., Smartt, S. J., & Danziger, I. J. 2005, MNRAS, 364, L33
Müller, E., Fryxell, B., & Arnett, D. 1991, A&A, 251, 505
Nadyozhin, D. K. 2003, MNRAS, 346, 97
Pastorello, A., Sauer, D., Taubenberger, S., et al. 2006, MNRAS, 370, 1752
Pastorello, A., Della Valle, M., Smartt, S. J., et al. 2007, Nature, 449, 1
Prieto, J. L., Kistler, M. D., Thompson, T. A., et al. 2008, ApJ, 681, L9
Thorne, K. S., & Żytkow, A. N. 1975, ApJ, 199, L19
Tsvetkov, D. Yu., Volnova, A. A., Shulga, A. P., et al. 2006, A&A, 460, 769
Utrobin, V. P. 2004, Astron. Lett., 30, 293
Utrobin, V. P. 2005, Astron. Lett., 31, 806
Utrobin, V. P. 2007, A&A, 461, 233
Utrobin, V. P., Chugai, N. N., & Pastorello, A. 2007, A&A, 475, 973
Van Dyk, S. D., Peng, C. Y., King, J. Y., et al. 2000, PASP, 112, 1532
Vink, J. S., de Koter, A., & Lamers, H. J. G. L. M. 2001, A&A, 369, 574
Woosley, S. E. 1988, ApJ, 330, 218